




Research Article

Use of a Full Factorial Design to Study the Relationship between Water Absorption and Porosity of GP and BW Mortar Activated

Nadia Tebbal ¹, Mekki Maza ², and Zine El Abidine Rahmouni ²

¹Institute of Technical Urban Management, M'sila University, M'sila 28000, Algeria

²Geo-materials Development Laboratory, Civil Engineering Department, Faculty of Technology M'sila University, M'sila 28000, Algeria

Correspondence should be addressed to Nadia Tebbal; nadia.tebbal@univ-msila.dz

Received 17 September 2022; Revised 11 November 2022; Accepted 28 November 2022; Published 12 December 2022

Academic Editor: Nikhil Saboo

Copyright © 2022 Nadia Tebbal et al. This is an open access article distributed under the Creative Commons Attribution License, which permits unrestricted use, distribution, and reproduction in any medium, provided the original work is properly cited.

The alkali-activated materials prepared by activation of glass powder (GP) and brick waste (BW) on the porosity and absorption of geopolymer paste by alkaline solution (alkali + water glass) were investigated. The effect of the combination of GP and BW on the porosity and absorption of the prepared geopolymer paste was monitored and evaluated by both laboratory and analytical methods. In this paper, three mortars were made with two sources of geopolymer containing 100% BW and 100% GP and blended with 90% GP and 10% BW replacements by mass. The compressive strength, porosity, and absorption of alkali-activated mortar were concurrently examined. Furthermore, the laboratory results obtained were estimated by the general full factorial design method. Finally, the analysis of variance was performed using the test results to analyze the importance of the effect factors and their interactions on the selected responses. The results concluded that mortar activated combined with 10% BW and 90% GP could be utilized in the industry of construction with minimum pollution problems and environment-friendly building materials, with the effect variables significantly affecting the responses.

1. Introduction

Ordinary Portland cement is one of the most polluting products in terms of CO₂ emissions. However, the concrete industry has implemented several mechanisms to reduce the CO₂ emissions, but they have had only a very minimal effect [1]. The sustainability approach, focusing on green consumption of discarded materials and suppressing climate change, is an appropriate solution to environmental degradation. Thus, it has been developed in a systematic way for all new products from the waste generated from all industrial and construction activities [2]. Alkali-activated binders are getting a lot of consideration because of their strong resistance, durability, and low environmental impact [3, 4]. Recent studies have proven that the gases that cause global warming can be reduced by up to eighty percent by using alkaline concrete compared to Portland cement [5].

Alkali activation technology is one of the modern techniques that tries to a large extent to reduce the use of ordinary concrete (OPC). A new cement-free binder for making concrete has appeared as a replacement for OPC [6]. Using industrial waste products such as alkali-activated blast furnace slag, BW, and GP can be considered as substitute binders for OPC. The amorphous to semicrystalline three-dimensional silico-aluminate structures of the poly(sialate) type (-Si-O-Al-O-) or of the poly(sialate-siloxo) type (-Si-O-Al-O-Si-O-) were named “geopolymers” by Davidovits [7]. In recent studies, the mineral additives (metakaolin, clay, fly ash, and slag) have been given great importance in terms of activating alkali [8].

Reig et al. [9], in their study, proved that the mortar reached a compressive strength of 30 MPa after a short term with SiO₂: Na₂O ratio = 1.60. Rakhimova and Rakhimov justified that the use of alkaline activated from granulated slag (S) with lot of percentages by BW and three solutions of

Na_2SiO_3 , NaOH , and Na_2CO_3 , the mechanical behavior of mixture with S/BW ratio 60/40 was higher than for one-component binders and reached 120 MPa when S and BW were milled together [10].

Sedira and Castro-Gomes studied an alkali-activated binder based on tungsten clay and BW residues. This study showed that the increase in the rate of BP between the rate of 10 to 50 percent is accompanied by an increase in the mechanical resistance, from 25 to 59 MPa, for all ages tested [11]. Concrete is a porous material that has water permeability properties, which have an impact on its strength as well as its durability. Via a chemical reaction between water molecules and cement, hydrates containing C-S-H and $\text{Ca}(\text{OH})_2$, and porosity with various pore distribution which are produced in the manner can be the main route of water and gas. The processing condition and type of mixture ratios and mineral additives on the relevant porosity have been studied by much research although the relationship between porosity and durability of concrete was not given an accurate explanation [12].

Other studies indicated that there was an increase in compressive strength with an increase in NaOH concentration. Hence, the percentage of water absorption was also decreased with an increase in NaOH concentration and curing time [13], especially for the performance of the brick-based geopolymers [14]. The researchers chose to use the optimum concentration of NaOH between 8 and 12 M, at which the geopolymer exhibits the best mechanical properties [15, 16].

This paper investigates the relation between water absorption and porosity of mortar activated by GP and BW by an experimental method and then evaluates it by an analytical method.

2. Materials and Methods

2.1. Materials. Geopolymer mixtures have been made from Glass Powder (GP) and Brick Waste powder (BW) as aluminosilicate precursors, and modified sodium water glass was used as an alkaline activator. The characteristics of all materials used are shown below:

Glass powder (GP): the waste beverage glass was used for this study. The glass was then ground to the point of obtaining the Blaine fineness of $1960 \text{ cm}^2/\text{g}$ and specific gravity equal to 2.61.

Brick waste (BW): remains of brick were obtained from building debris, which was crushed in a laboratory mill. The WB powder has a density of 2.55 and a Blaine fineness of $3036 \text{ cm}^2/\text{g}$.

Sand: standardized sand using for all mortars and conforming to the EN 196-1.

The alkaline activator solution: the alkaline activator used in this study was a combination of Na_2SiO_3 and NaOH . The NaOH has a granular shape and is distinguished by its purity 100.5% and 10 M solution was fixed. The upper limit of NaOH was restricted as 10 M, to maintain minimum workability [18]. The Na_2SiO_3

consisted of 10.6% Na_2O , 26.5% SiO_2 , and 62.9% H_2O (with specific gravity of 1.39 at 20°C and $\text{SiO}_2/\text{Na}_2\text{O}$ weight ratio of 3). The properties of the materials used are shown in Table 1.

2.2. Preparation of Mortar Samples. Strengthening bonds activated by alkali, GP and BW materials were mixed with an alkaline solution. GP and BW were used at proportions of GP: BW-waste of 0:100, 90:10, and 100:00 by weight. Therefore, these mortars were designed as M GP, M BW and M GP90 WB10. These doses were chosen on the basis of the Tebbal et al.'s study [18, 19].

Mortars were formulated with 1 : 3 proportions of GP and standard sand. For the mixing procedure, the activator solution was mixed with the filler for 5 min in a pan mixer, and then the sand added and mixed for 5 min. Finally, the remaining activated solution; continue mixing for another 5 minutes. This mixing procedure was test and found to produce high strength geopolymer. After mixing, it was poured into $2.5 \text{ cm} \times 2.5 \text{ cm} \times 2.5 \text{ cm}$ molds, which were then subjected to a precured treatment that consisted of subjecting them to a relative humidity of 100%, with a temperature of 40°C and for a period of 24 hours. Next curing at this temperature, the mortars were put in laboratory to cool down and demoulded next day to keep them in until testing age. The specimens were tested at the age of 7, 14 and 28 days.

Strength, porosity, and absorption test: the mortar compressive strengths test were determined using prismatic specimens of square section $2.5 \text{ cm} \times 2.5 \text{ cm}$ and length 10 cm in accordance with EN 196-1.

The protocol of porosity accessible to water conform the recommendations of AFREM group [20]. The test pieces for testing of water porosity are dried in an oven at a temperature of 100°C to constant weight and then returned to room temperature in a desiccator.

The porosity test is carried out on test pieces of dimensions $2.5 \text{ cm} \times 2.5 \text{ cm} \times 2.5 \text{ cm}$, by applying the following steps [21]:

- (1) Drying in an oven at 105°C of the sample for at least 24 hours until obtaining a constant mass. Then, they were weighed once dry (A);
- (2) Immersion of the sample in water for 24 hours;
- (3) Heating to boiling for 5 hours, then weighing the sample in air (weight "C");
- (4) Finally, hydrostatic weighing (D: weight of saturated samples subjected to Archimedes).

The porosity was calculated by the following formula:

$$P(\%) = \frac{(C - A)}{(C - D)} 100. \quad (1)$$

The water-absorption test was performed in accordance with ASTM C140/C140M-18 [22] to determine the porosity of the samples. The sample masses were measured before and after immersion in water for 24 hours. Water absorption of samples was reported as the percentage increase in weight.

TABLE 1: Chemical composition of GP and BW.

Compositions (%)	Glass powder (%)	Brick waste (%)
SiO ₂	71.96	62.54
CaO	9.26	8.78
Al ₂ O ₃	1.9	14.31
Fe ₂ O ₃	0.23	5.98
MgO	2.75	2.62
SO ₃	0.08	0.46
MnO	—	—
Na ₂ O	12.25	0.77
K ₂ O	0.28	2.01
Cl ⁻	0.007	0.026
PAF	1.29	2.5

Statistical study with factorial design approach (F.D.A): factorial designs allow estimating the effects of one factor at several levels of other factors, yield valid conclusions over a range of experimental conditions. It allows an optimum assessment of the main and interaction effects among the independent effect variables named factors “*xi*” and the outcome variables named responses “*Y*” [23].

To evaluate the relationship between water absorption and porosity of glass powder and brick waste mortar activated, an experimental factorial design was performed. The analysis of variance (ANOVA) has been used to study the effects of different factors considered and their interactions [24] and the results were evaluated and analyzed by using JMP16 software. Figure 1 presented the flowchart related to the steps followed by the F.D.A.

3. Results and Discussion

3.1. Compressive Strength. Compressive strengths of geopolymers prepared with variable glass powder and brick waste ratio are presented in Figure 2.

Strengths of all samples were rising over time until the age of 7, 14, and 28 days. Alkali-activated glass powder showed the highest short-term strengths (28 days). Brick powder geopolymer exhibited the lowest early strengths but after its combination with 90% GP, the values reached those observed for blends.

For the high strengths of the MGP mixtures, these results can be explained by the availability of the high amount of calcium and alumina in the mix leads to the formation of additional calcium silicate hydrate gel with high amounts of tetra-coordinated “Al” in its structure as well as “Na” ions in the interlayer spaces; hence, higher compressive strength is obtained [24, 25].

3.2. Water Absorption and Porosity. At 28 days, the water absorption and water accessible porosity of concrete with glass powder and brick waste are shown in Figures 3 and 4. The porosity of all mixtures MGP, MGP90BW10, and MBW increased with increasing glass powder content. On the other hand, there are improvements the absorption of water and porosity until the mixture formed by ninety percent of the glass powder and ten percent of the brick waste.

This reduction in water absorption is attributed to the pozzolanic reaction of glass powder, which can refine the pore structures and decrease the connectivity. As the brick waste content reaches 100%, the pozzolanic reaction would be limited by Portlandite, the cement hydration products. This agrees well with the lowest compressive strength for mortar with 100% BW.

The geopolymerization product produced by glass powder is less stable and increases the porosity due to the high amount of available alkalis present in the glass powder [18]. However, for the mix containing M GP90 BW 10 and M GP, the strength starts to increase as molar concentration 10 M. The availability of 10 M molar concentration with 90% GP and 10% BW may increase further the geopolymerization gel and increase the denseness of the matrix.

3.3. Modeling the Mechanical and Physical Characteristics. Figures below represent the observed values of the quadratic model as a function of the predicted values (that is, the relationship between the predicted area and the actual area measured).

3.3.1. Analysis and Results of the Model Variance. The compressive strength, coefficient of absorption, and porosity values were measured during the tests, which were compared with the results predicted by the quadratic model (Table 2). The values of R^2 and adj R^2 are close to 1(0.956–0.999), which improved the good correlation between the responses obtained experimentally and the model records.

The analyses of statistical parameters presented in Table 2 and Figures 5 and 6 indicate that the equations (2)–(6) represent adequately the actual relationship between the independent variables and the responses. The mathematical models used in the compressive strength, coefficient of absorption, and porosity test are given by the following equations:

$$R_{C7} = 14.308888889 + (-28.115) \left[\frac{(BW - 50)}{50} \right] + \left[\frac{(BW - 50)}{50} \right] \left[\frac{(GP - 50)}{50} \right] (-22.18611111), \quad (2)$$

$$R_{C14} = 15.93 + (-31.225) \left[\frac{(BW - 50)}{50} \right] + \left[\frac{(BW - 50)}{50} \right] \left[\frac{(GP - 50)}{50} \right] (-24.625), \quad (3)$$

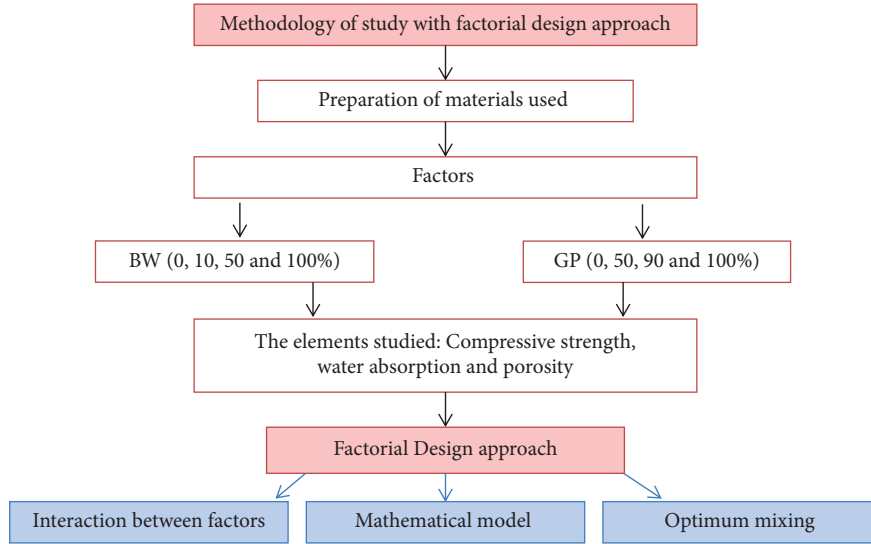


FIGURE 1: Flowchart related to the steps followed by the F.D.A.

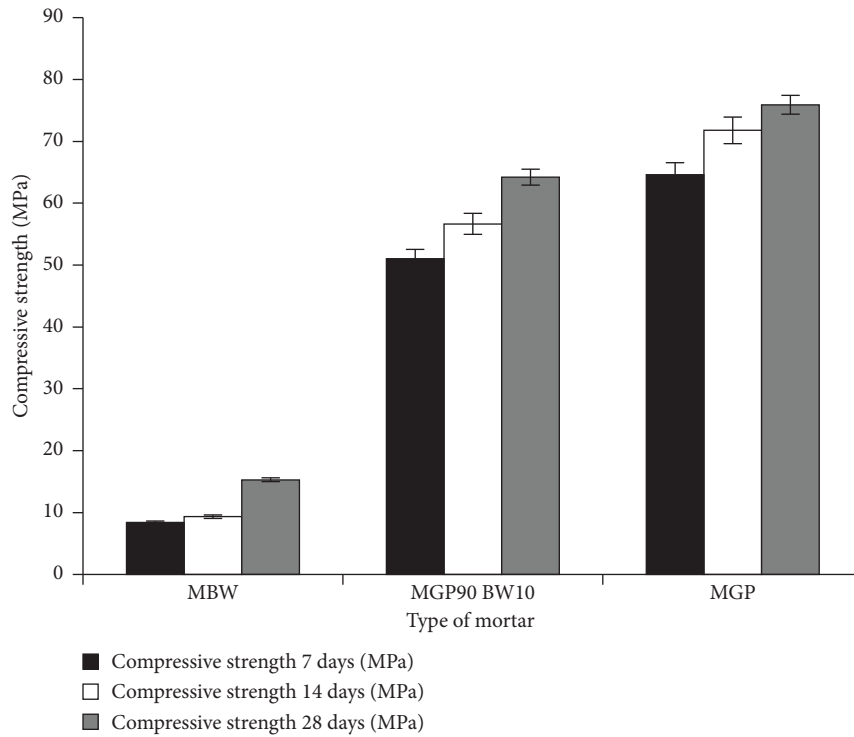


FIGURE 2: Compressive strengths of prepared geopolymer mortars.

$$R_{C28} = 29.95111111 + (-30.305) \left[\frac{(BW - 50)}{50} \right] + \left[\frac{(BW - 50)}{50} \right] \left[\frac{(GP - 50)}{50} \right] (-15.66388889), \quad (4)$$

$$\text{Absorption coefficient (28 days)} = 10.228307544 + 1.9263249516 \left[\frac{(BW - 50)}{50} \right] + \left[\frac{(BW - 50)}{50} \right] \left[\frac{(GP - 50)}{50} \right] (-2.794532495), \quad (5)$$

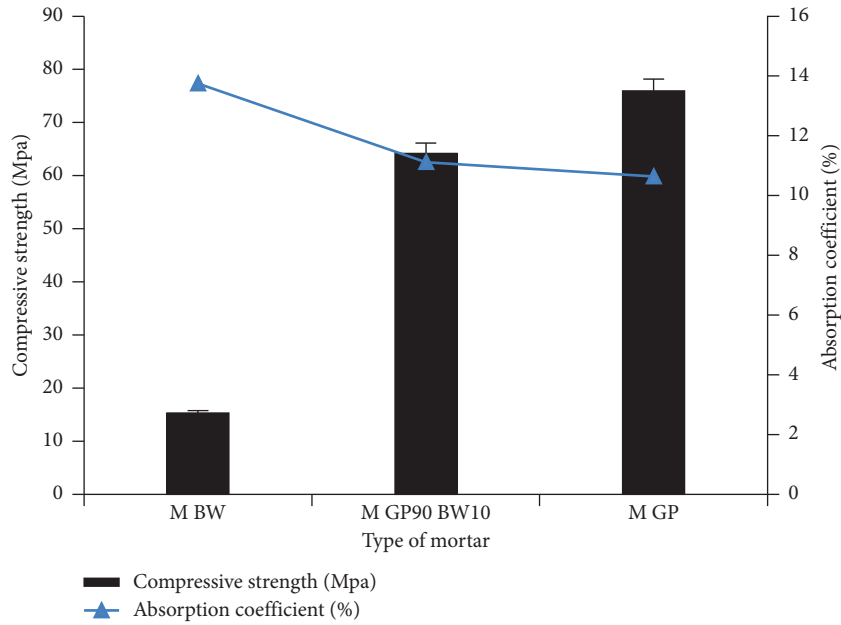


FIGURE 3: Water absorption of mortar at the age of 28 days.

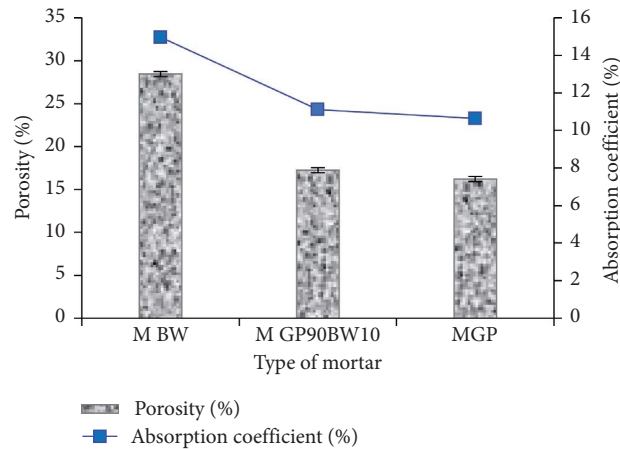


FIGURE 4: Porosity and water absorption of mortar at the age of 28 days.

TABLE 2: Summary of fit.

	RC 7	RC 14	RC 28	Water absorption	Porosity
R^2	1	0.990	1	0.98	0.98
Adjusted R^2	0.881	0.950	0.999	0.869113	0.886042
RMSE	2.2135	5.0505	0.5834	0.3713	0.8756
Mean of response	33.63	52.13	49.885	11.6875	18.975

RC 7: compressive strength at 7 days, RC 14: compressive strength at 14 days, RC 28: compressive strength at 28 days.

$$\text{Porosity (28 days)} = 14.61032882 + 5.4418568665 \left[\frac{(BW - 50)}{50} \right] + \left[\frac{(BW - 50)}{50} \right] \left[\frac{(GP - 50)}{50} \right] (-8.262185687). \quad (6)$$

The plotted between residuals and predicted response for compressive strength at 7 (a), 14 (b), 28 days (c), absorption water (d), and porosity (e) at 28 days in order to test the

hypothesis of constant variance has shown in Figure 6. We clearly note that scattering random (i.e., without geometrical shape) explains why the assumption is not violated.

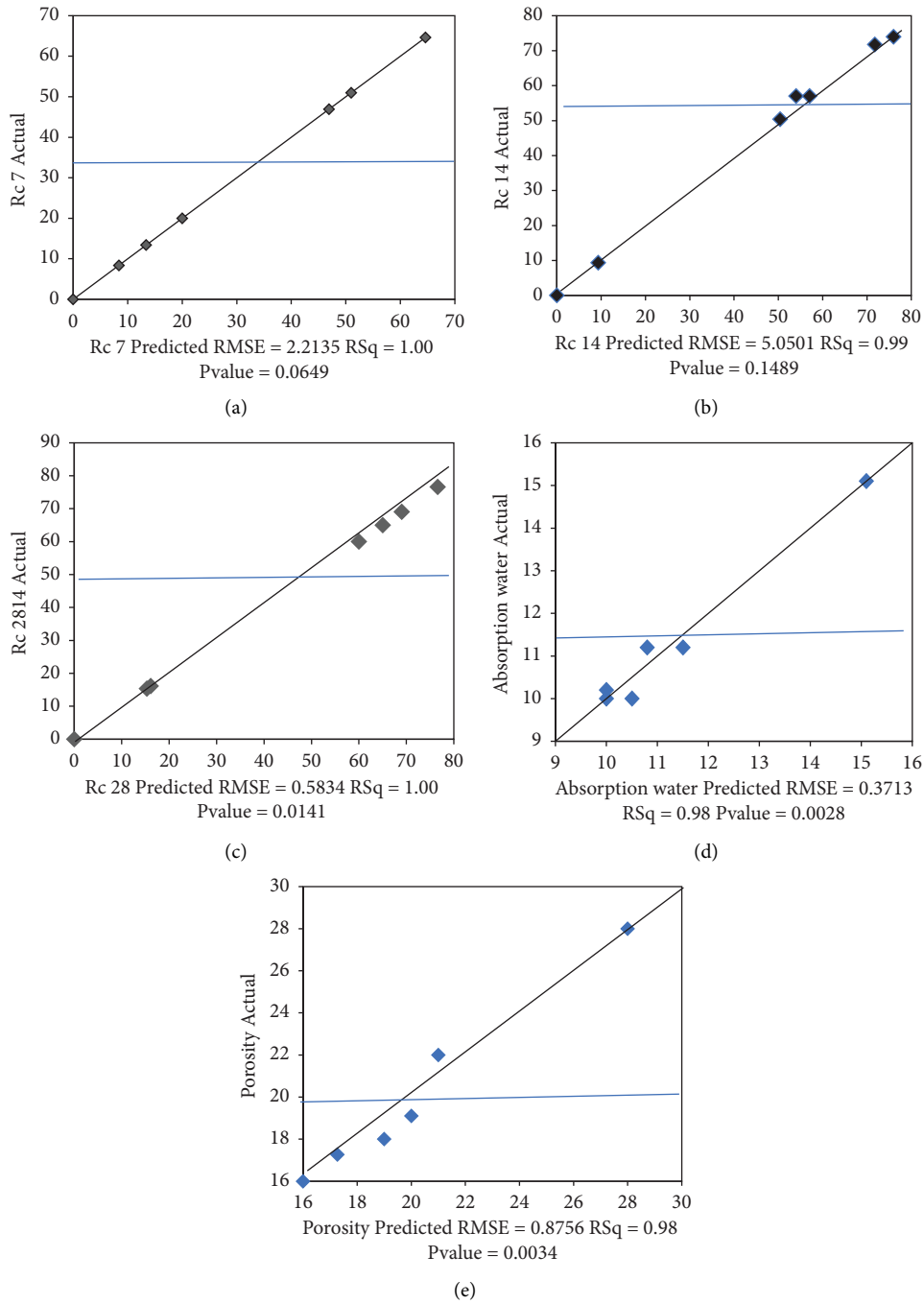


FIGURE 5: Correlation between the observed and predicted responses (RC7 (a), RC14 (b), RC28 (c), water absorption (d), and porosity (e)) at 28 days.

3.3.2. *Compressive Strength, Water Absorption, and Porosity Results Analysis.* The following Figure 7 shows the different types of plots resulting from the analysis of compressive strength results at 7, 14, and 28 days and water absorption with porosity, taking GP (mass%) and BW (mass%) factors into account.

3.4. *Compressive Strength.* Figures 7 (a)–7 (c) shows clearly that compressive strength is following a linear relationship with the % mass of brick waste and their combination with glass powder. A higher slope of surface load shows its stronger effect on GP in comparison to BW. From the iso-response surfaces of the compressive strengths, it can be

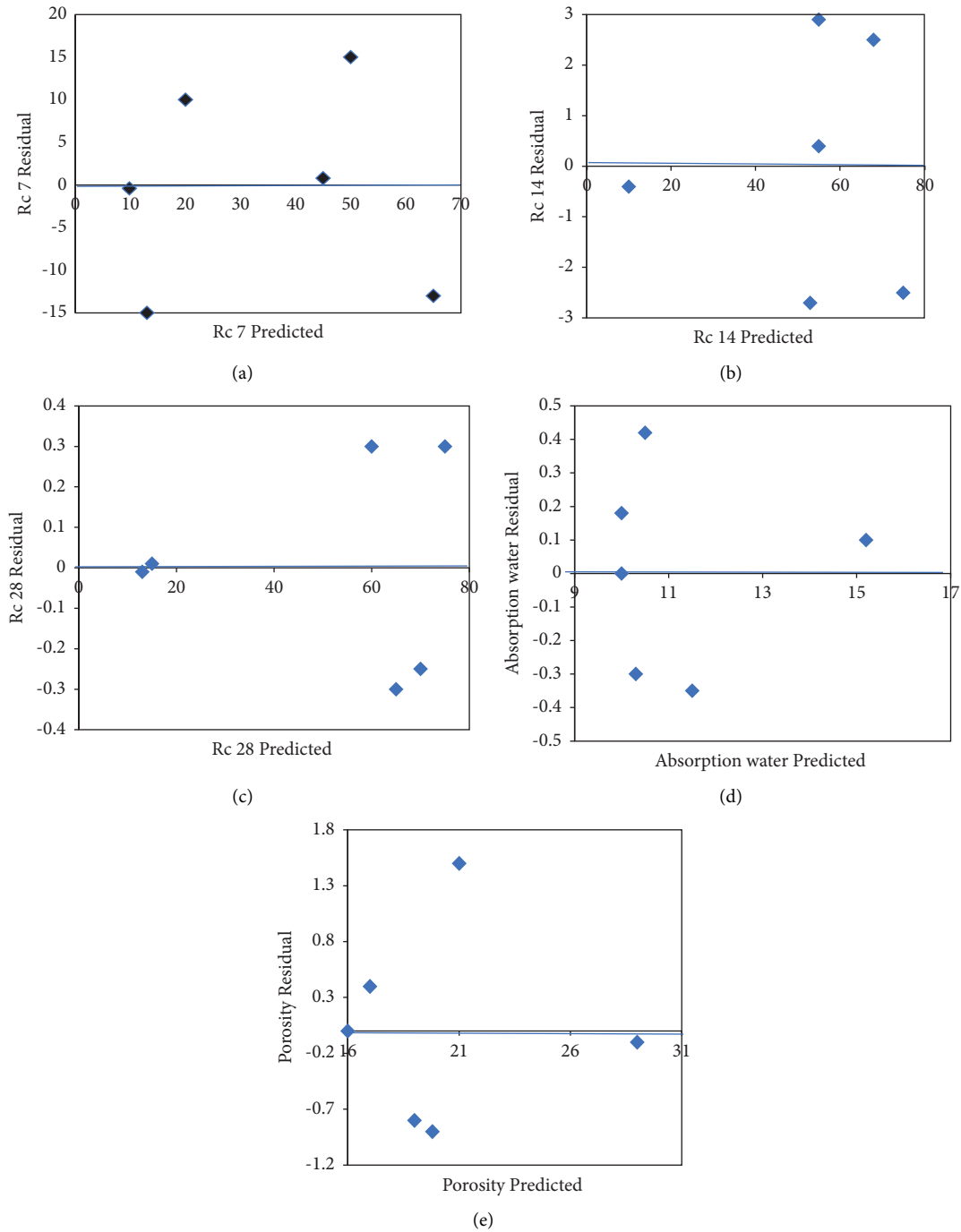


FIGURE 6: The residual values according to the predicted values of RC7 (a), RC14 (b), RC28 (c), water absorption (d), and porosity (e) at 28 days.

clearly deduced that the minimum mechanical strength has been reached at the lower BW level. Also, the maximum resistance occurred for the conditions when GP levels were at their maximum. The flat profile of model surfaces for resistance shows that the best fitted model is linear in nature.

3.5. Water Absorption and Porosity. Figures 7(d) and 7(e) determine the effect of two factors (BW mass %) and (GP mass %) on the water absorption and porosity responses at 28 days.

It is observed that the % contains of GP played an important role in porosity and water absorption of the mortar to 10.64% and 16.21%, respectively. On the other

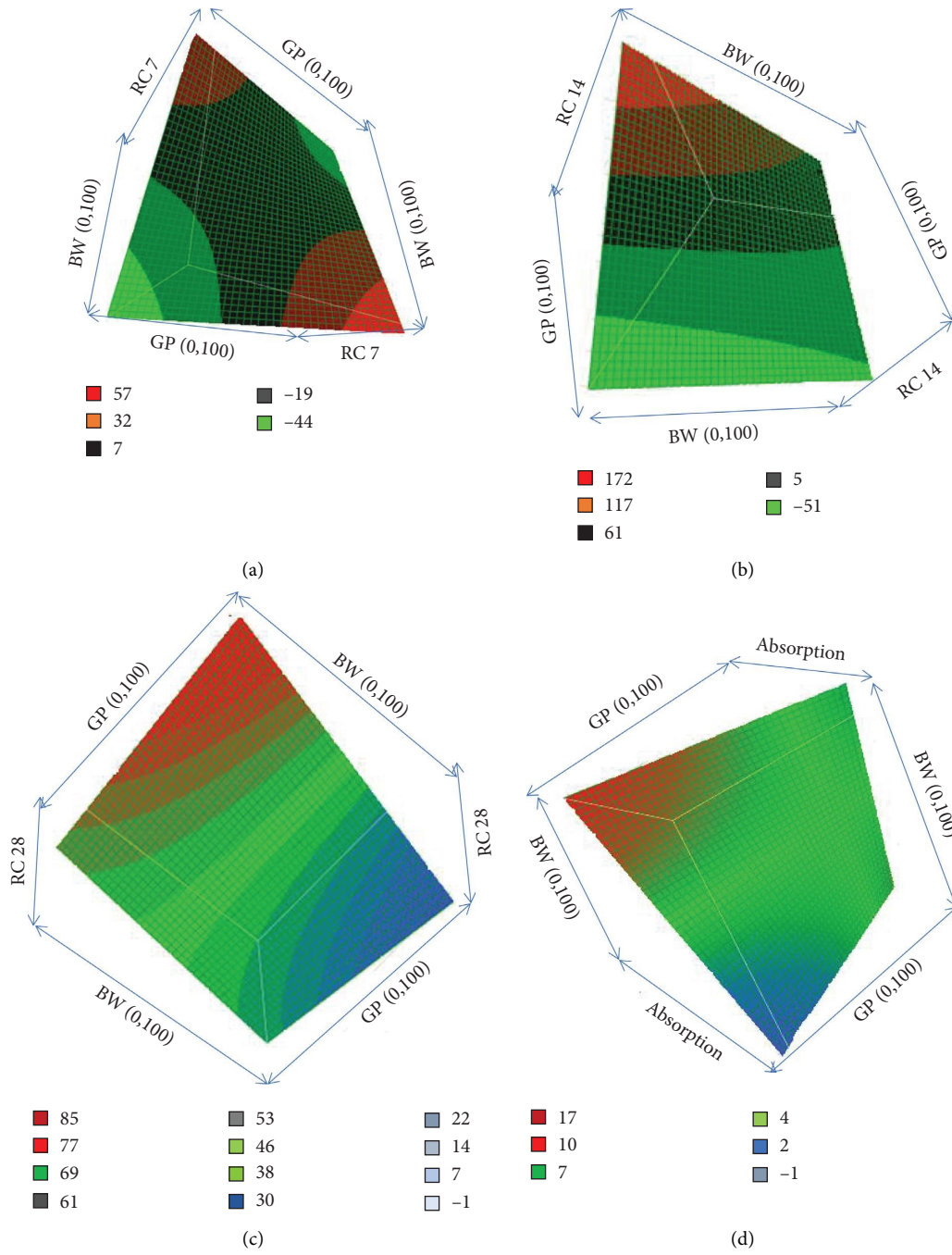


FIGURE 7: Continued.

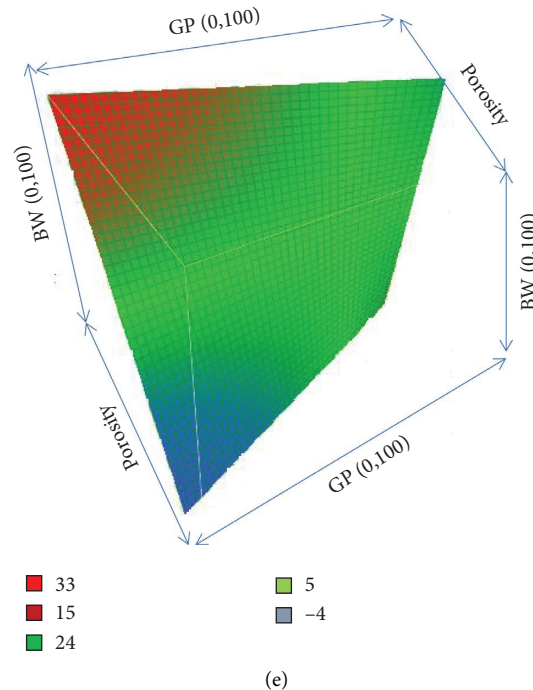


FIGURE 7: Isoresponse surfaces of the compressive strengths at 7, 14, and 28 days, and water absorption with porosity.

hand, increasing the brick waste content to 100% caused an increase in water absorption and porosity. Moreover, the mixture containing 10% BW and 90% GP presented less water absorption of 11.11% and 17.24% porosity as compared to the mixture made with 100% BW.

These results are consistent with the estimated coefficient equation (5), where the coefficients of the BW and the interaction between BW and GP content are (1.9263249516) and (-2.794532495), respectively. Therefore, the effect of BW (GP) is greater than the effect of BW (%) on absorption at 28 days. Also, equation (6) showed the effect of porosity, which follows the same trend as absorption.

4. Conclusions

From the above experimental results, the following conclusions are drawn:

The highest compressive strength of glass powder-based geopolymer concrete mortar can be achieved at 64.22 MPa at 28 days when GP 90% and BW 10% are used. However, the highest compressive strength of reference mortar was 76.0 MPa at 28 days with mortar at 100% GP. Specimens produced with 100% (wt) brick obtained a lower resistance but still acceptable compressive strength value (15.31 MPa). The porosity of the geopolymer mortar combined with the brick waste and glass powder increased with increasing glass powder content. The absorption of glass powder-based geopolymer mortar (11.11%) is lower than M WB (14.97%), but still comparable to the properties of M GP90 BW10

mortar. The effect of GP content and of BW on the responses studied was clearly presented by isoresponse curves, and the full factorial design offers a new equation that can be proposed for the prediction of 7, 14, and 28 day compressive strengths, porosity, and water absorption.

This research concludes that geopolymer glass bricks (GP 90%; BW 10%) are an environment-friendly alternative to conventionally fired bricks.

Finally, we noticed that most studies focused on the economic impact as well as durability properties of geopolymer bricks through alkali activation methods, but CO₂ treatment of fresh concrete or mortar, such as carbon capture and storage, can be a solution to the high cost problem.

Data Availability

All the data are included in the manuscript from the corresponding author upon request.

Conflicts of Interest

The authors declare that they have no conflicts of interest.

Acknowledgments

The authors thank the Geo-Materials Development Laboratory (M'sila University) and Directorate of Scientific Research and Technological Development (DGRSDT-MESRS, Algeria) for the assistance and support to complete this paper.

References

- [1] P. Duxson and J. Provis, "Low CO₂ concrete: are we making any progress?" *Environment Design Guide*, vol. 24, pp. 1–7, 2008.
- [2] P. Awoyera and A. Adesina, "Durability properties of alkali activated slag composites: short overview," *Silicon*, vol. 12, no. 4, pp. 987–996, 2020.
- [3] J. C. Liu, Z. Chen, R. Cai, and H. Ye, "Quantitative effects of mixture parameters on alkali-activated binder-based ultra-high strength concrete at ambient and elevated temperatures," *Journal of Advanced Concrete Technology*, vol. 20, no. 1, pp. 1–17, 2022.
- [4] M. C. G. Juenger, F. Winnefeld, J. L. Provis, and J. H. Ideker, "Advances in alternative cementitious binders," *Cement and Concrete Research*, vol. 41, no. 12, pp. 1232–1243, 2011.
- [5] P. Duxson, J. L. Provis, G. C. Lukey, and J. S. van Deventer, "The role of inorganic polymer technology in the development of "green concrete"," *Cement and Concrete Research*, vol. 37, no. 12, pp. 1590–1597, 2007.
- [6] G. F. Huseien, J. Mirza, M. Ismail, S. K. Ghoshal, and A. A. Hussein, "Geopolymer mortars as sustainable repair material: a comprehensive review," *Renewable and Sustainable Energy Reviews*, vol. 80, pp. 54–74, 2017.
- [7] J. Davidovits, *Geopolymer Chemistry and Application*, Institut Géopolymère, Morrisville, France, 2008.
- [8] P. Rovnanik, B. Řezník, and P. Rovnaníková, "Blended alkali-activated fly ash/brick powder materials," *Procedia Engineering*, vol. 151, pp. 108–113, 2016.
- [9] L. Reig, M. M. Tashima, M. V. Borrachero, J. Monzó, C. R. Cheeseman, and J. Payá, "Properties and microstructure of alkali-activated red clay brick waste," *Construction and Building Materials*, vol. 43, pp. 98–106, 2013.
- [10] N. R. Rakhimova and R. Z. Rakhimov, "Alkali-activated cements and mortars based on blast furnace slag and red clay brick waste," *Materials & Design*, vol. 85, pp. 324–331, 2015.
- [11] N. Sedira and J. Castro-Gomes, "Study of an alkali-activated binder based on tungsten mining mud and brick powder waste," in *Proceedings of the MATEC Web of Conferences*, France, July 2018.
- [12] M. N. Qureshi and S. Ghosh, "Effect of curing conditions on the compressive strength and microstructure of alkali-activated GGBS paste," *International Journal of Engineering Science Invention*, vol. 2, no. 2, pp. 24–31, 2013.
- [13] Z. Xu, J. Yue, G. Pang, R. Li, P. Zhang, and S. Xu, "Influence of the activator concentration and solid/liquid ratio on the strength and shrinkage characteristics of alkali-activated slag geopolymer pastes," *Advances in Civil Engineering*, vol. 2021, Article ID 6631316, 11 pages, 2021.
- [14] D. Kioupis, A. Skaropoulou, S. Tsvilis, and G. Kakali, "Valorization of brick and glass CDWs for the development of geopolymers containing more than 80% of wastes," *Minerals*, vol. 10, no. 8, p. 672, 2020.
- [15] R. M. Hamidi, Z. Man, and K. A. Azizli, "Concentration of NaOH and the effect on the properties of fly ash based geopolymer," *Procedia Engineering*, vol. 148, pp. 189–193, 2016.
- [16] N. Youssef, A. Z. Rabenantoandro, Z. Dakhli et al., "Reuse of waste bricks: a new generation of geopolymer bricks," *SN Applied Sciences*, vol. 1, no. 10, pp. 1–10, 2019.
- [17] En, *Methods of testing cement - Part 1: Determination of strength*, 2018.
- [18] N. Tebbal and Z. E. A. Rahmouni, "Recycling of brick waste for geopolymer mortar using full factorial design approach," *The Eurasia Proceedings of Science Technology Engineering and Mathematics*, vol. 7, pp. 44–47, 2019.
- [19] C. L. Hwang, M. D. Yehualaw, D. H. Vo, T. P. Huynh, and A. Largo, "Performance evaluation of alkali activated mortar containing high volume of waste brick powder blended with ground granulated blast furnace slag cured at ambient temperature," *Construction and Building Materials*, vol. 223, pp. 657–667, 2019.
- [20] Afpc-Afrem, "Groupe de travail Durabilité des bétons. Recommended test methods for measuring the parameters associated to durability," *Proceedings des Journées Techniques AFPC-AFREM: Durabilité des Bétons*, 1998.
- [21] N. Tebbal, Z. Rahmouni, and M. Maza, "Combined effect of silica fume and additive on the behavior of high performance concretes subjected to high temperatures," *Mining Science*, vol. 24, 2017.
- [22] Astm C140 C140M 17, *Standard Test Methods for Sampling and Testing Concrete Masonry Units and Related Units*, ASTM International, West Conshohocken, PA, USA, 2017.
- [23] K. Gelis, K. Ozbek, A. N. Celik, and O. Ozyurt, "A novel cooler block design for photovoltaic thermal systems and performance evaluation using factorial design," *Journal of Building Engineering*, vol. 48, Article ID 103928, 2021.
- [24] D. C. Montgomery, *Design and Analysis of Experiments*, Wiley, Hoboken, 2017.
- [25] S. R. Salla, C. D. Modhera, and U. R. Raghu Babu, "An experimental study on various industrial wastes in concrete for sustainable construction," *Journal of Advanced Concrete Technology*, vol. 19, no. 2, pp. 133–148, 2021.